

of the x-ray production cross sections indicate they are correct to 20 percent or better for all four elements. The total L -shell ionization cross sections σ_{LI} , listed in column 5 of Table II, are obtained by correcting σ_{LX} for Auger transitions. The Auger factors are not too well known; those used were the ones obtained by Lay in 1934 and given by Burhop.⁵

Table II includes for comparison some K -shell

⁵ E. H. S. Burhop, *The Auger Effect* (Cambridge University Press, Cambridge, 1952), p. 55.

ionization cross sections σ_{KI} , taken from reference 2. These are smaller than the L -shell cross sections by several orders of magnitude. The L -shell cross sections do not fit simple power laws in either proton-energy or atomic-number dependence; however, the variation is slower in both respects than the approximately E^4/Z^{12} dependence of the K shell.

We wish to thank Dr. E. Merzbacher for many helpful discussions of the theory and for his continuing interest in this work.

Decay Scheme and Gamma-Gamma Correlations in $B^{10}\dagger$

S. M. SHAFROTH* AND S. S. HANNA

Department of Physics, The Johns Hopkins University, Baltimore, Maryland

(Received March 18, 1954)

Gamma rays from the deuteron bombardment of beryllium were studied with two scintillation spectrometers operated in coincidence. Gamma rays of energies 2.86, 2.15, 1.43, 1.02, 0.72, and 0.41 Mev, which have previously been associated with the B^{10} nucleus, were identified in single-channel spectra. Coincidences were observed between the following pairs of gamma rays: 2.86–0.72, 2.15–1.43, 1.43–1.43, 1.43–1.02, 1.43–0.72, 1.43–0.41, 1.02–0.72, 1.02–0.41, and 0.72–0.41. The decay scheme obtained from these measurements agrees with the one proposed by Ajzenberg, except for the presence of an additional 1.43-Mev transition between the 3.58- and 2.15-Mev states of B^{10} . A survey was made of the directional angular correlations between several of these coincident radiations.

I. INTRODUCTION

THE gamma rays emitted in the $Be^9(d,n)B^{10*}(\gamma)B^{10}$ reaction have been investigated by Rasmussen *et al.*¹ with a spectrometer of high resolution. From measurements on the energies of the neutron groups, Ajzenberg² has determined the excitation energies of the states in B^{10} and has deduced a decay scheme which would account for all the observed gamma rays. The excitation energies have also been obtained by Pruitt *et al.*³ and Dyer and Bird⁴ from observations of the neutron groups in the same reaction, and by Bockelman *et al.*⁵ from the inelastic scattering of protons and deuterons by B^{10} nuclei.

In order to establish the decay scheme directly and to investigate some of the gamma-gamma angular correlations, we have searched for coincidences between all possible pairs of gamma rays emitted by the B^{10} nucleus in the Be^9+d reaction at bombarding energies below 0.7 Mev.

[†] Assisted by a contract with the U. S. Atomic Energy Commission.

* Now at Northwestern University, Evanston, Illinois

¹ Rasmussen, Hornyak, and Lauritsen, *Phys. Rev.* **76**, 581 (1949); V. K. Rasmussen, Ph.D. thesis, California Institute of Technology, 1950 (unpublished).

² F. Ajzenberg, *Phys. Rev.* **82**, 43 (1951); *Phys. Rev.* **88**, 298 (1952).

³ Pruitt, Swartz, and Hanna, *Phys. Rev.* **92**, 1456 (1953).

⁴ A. J. Dyer and J. R. Bird, *Australian J. Phys.* **6**, 45 (1953).

⁵ Bockelman, Browne, Sperduto, and Buechner, *Phys. Rev.* **90**, 340 (1953); **92**, 665 (1953).

II. APPARATUS

A thick target of beryllium was bombarded with deuterons from an electrostatic accelerator. The target was located at the center of a cylindrical target chamber, 3 inches in diameter. The brass wall of the chamber was $\frac{1}{2}$ inch thick.

The spectrum of the gamma radiation was studied with a scintillation spectrometer consisting of a cylindrical, sodium iodide crystal, 2 inches long, 1.5 inches in diameter, packed in magnesium oxide powder,⁶ and mounted on an RCA 5819 photomultiplier tube. The pulses from the phototube passed through a cathode follower, a linear amplifier, and then were analyzed in a single channel differential analyzer.

For the coincidence work a second scintillation spectrometer was used in coincidence with the first. The second system was similar in every way to the first, except that the crystal was 1.25 inches long. The pulses from the two analyzers operated blocking oscillators which presented uniform pulses to a 6AS6 tube for coincidence analysis. Accidental coincidences were monitored with a separate coincidence circuit, which received delayed pulses from one analyzer and undelayed pulses from the other.

⁶ C. J. Borkowski and R. L. Clark, *Rev. Sci. Instr.* **24**, 1046 (1953).

III. GAMMA RADIATION FROM B^{10}

The counters were calibrated with gamma rays of known energy from radioactive sources. A typical calibration is given in Fig. 1. A knowledge of the spectrum of the ThC'' gamma ray (2.62 Mev), which depends on the crystal geometry, aided in untangling the complex spectrum from the Be^9+d reactions. For the high-energy gamma rays identified in Fig. 2, the positions of the three main pair peaks and the Compton maximum are indicated. The 3.36-Mev gamma ray is attributed to Be^{10} , the 2.86, 2.15, 1.43, 1.02, and 0.72-Mev gamma rays to B^{10} .^{1,7} Figure 3 shows the low energy spectrum. The structure at 0.48 Mev is

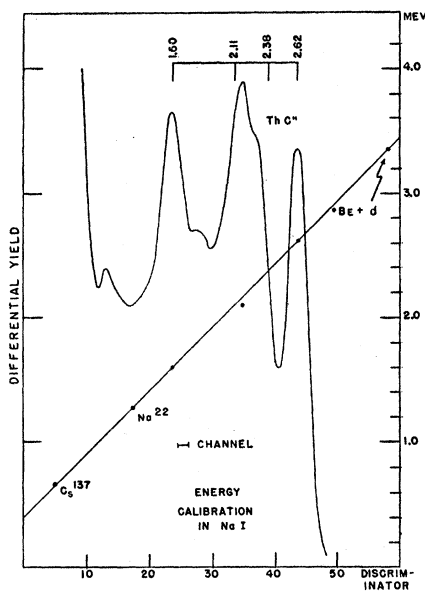


FIG. 1. Energy calibration of the 2-inch long NaI crystal and the pulse-height spectrum of the ThC'' (2.62-Mev) gamma ray. The vertical lines at the top locate the two-escape pair peak, the one-escape peak, the upper edge of the Compton distribution, and the no-escape (plus photo) peak. The one-escape pair peak is distorted by the Compton structure. The points labeled Cs^{137} and Na^{22} give the location of the photopeaks of the corresponding 0.67- and 1.28-Mev radiation. The points labeled Be^9+d show the location of the two highest recorded peaks, at 3.36 and 2.86 Mev, in the gamma-ray spectrum from Be^9+d (see Fig. 2).

attributed to the Li^7 gamma ray, the peak at 0.41 Mev to a B^{10} gamma ray. The structure in this region, however, was not very reproducible because of the presence of some annihilation radiation resulting from the bombardment of carbon impurity on the target.

IV. COINCIDENCE SPECTRA

The coincidence spectra were obtained by keeping the channel of one detector fixed on a peak in the spectrum and moving the channel of the other detector through the region of interest, while recording the

⁷ The weak 3.58-Mev gamma ray is not apparent in these spectra, but no special effort was made to resolve it.

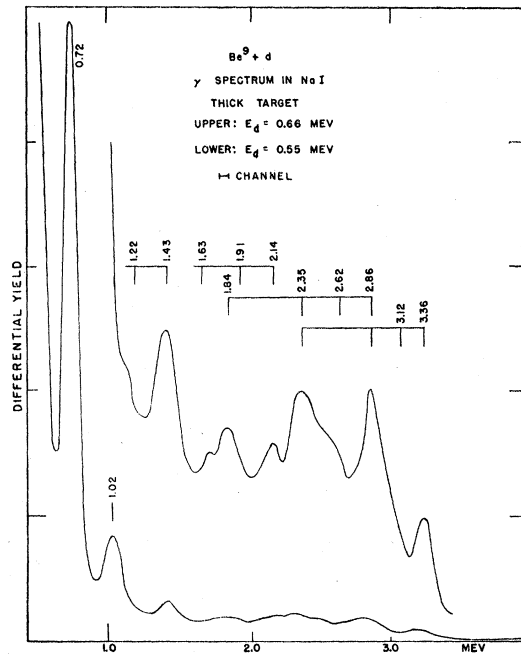


FIG. 2. Two spectra of the high-energy gamma rays from the Be^9+d reactions. The ordinates of the two curves are in the ratio of approximately 10:1. There is also a slight shift in the abscissas of the two spectra. The energy scale applies to the lower spectrum. The vertical lines locate the three pair peaks and the Compton edge of the various gamma rays. Above 3.0 Mev the energy scale is nonlinear because of overloading in the amplifier.

coincidence yield. Total yields and coincidence yields were normalized to the count in the fixed channel. In order to obtain sufficient intensity, most of the coincidence runs were made with fairly wide channels (3 to 8 volts). Because of the overlapping structure

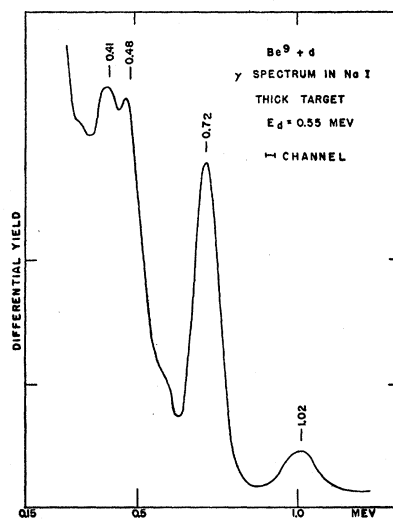


FIG. 3. Spectrum of the low-energy gamma rays from the Be^9+d reactions. In the region of 0.5 Mev there is a small contribution of annihilation radiation arising from the positron decay of N^{13} produced by deuteron bombardment of C^{12} .

of the various gamma rays, it is, in general, difficult to make quantitative comparisons of relative intensities in these spectra. In some instances the intensities were also affected by the fact that for wide variations of the channel setting the coincidence efficiency of the circuit was not constant.

A. Spectrum in Coincidence with 2.86-Mev Radiation

Figure 4 shows the coincidence spectrum and single channel spectrum when the channel of one counter was set on the 2.86-Mev peak, and the channel of the other counter was varied through the region from 0.4 to 3.0 Mev. Comparing the coincidence spectrum with the total spectrum, it is seen that the only detectable coincidence response occurs at and below the 0.72-Mev peak. Figure 8 shows the low-energy spectrum obtained with the 2.86-Mev setting. From this figure it appears that the 0.41-Mev gamma ray is not detectably in coincidence with the 2.86-Mev gamma ray, since the response in this region can be attributed to the Compton structure from the 0.72-Mev gamma ray.

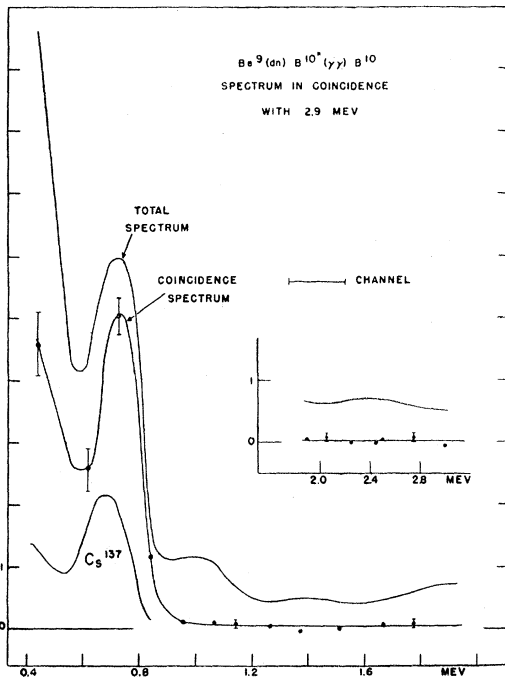


FIG. 4. The total spectrum shows the total yield obtained as a function of discriminator setting, using the wide (7.5-volt) channel shown. The coincidence spectrum, obtained simultaneously, shows the yield in coincidence with pulses in a fixed channel of the other counter. The fixed channel was set to receive pulses corresponding to energies between 2.55 and 3.05 Mev, i.e., on the 2.86-Mev peak. The energy scale was obtained from a calibration similar to Fig. 1. For comparison the Cs^{137} gamma-ray spectrum is shown, taken under the same conditions as the total spectrum. The vertical scales are arbitrary and of course different for the three spectra.

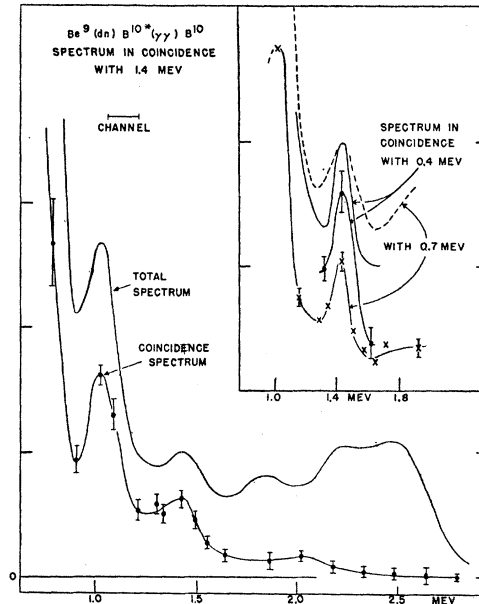


FIG. 5. Total spectrum and coincidence spectrum with the fixed channel of the other counter set on the 1.43-Mev peak. In the inset the dotted curve and the crosses give the total spectrum and coincidence spectrum, respectively, with the fixed channel on the 0.72-Mev peak. The solid curve and the dots were obtained with the fixed channel on the 0.41-Mev peak.

B. Spectrum in Coincidence with 1.43-Mev Radiation

Figures 5, 6, and 8 show the spectra obtained with the fixed channel set on the 1.43-Mev peak. In Fig. 5 a weak coincidence response in the region of 2 Mev is observed, indicating the existence of 1.43–2.15 Mev coincidences. In Figs. 5 and 6 there is evidence for 1.43–1.43 Mev coincidences, although the peak in this region can be attributed partially to 1.43–2.15 Mev coincidences. With both counters fixed on the 1.43-Mev setting, an increased response is expected, since both counters are also recording some 2.15-Mev radiation, and either gamma ray can count in either detector. At most, however, this response should be less than twice that for the 1.43–2.15 Mev setting, since 1.43 Mev does not correspond to a peak in the 2.15-Mev gamma spectrum. The pronounced 1.43–1.43 Mev response was also observed in a third run made independently.⁸ It is interesting that the energies of these two coincident gamma rays are so nearly the same that they were not resolved in the work of Rasmussen *et al.*¹

⁸ In evaluating these spectra, it is also necessary to consider the effect of two 0.72-Mev pulses occurring within the resolving time of a detector to produce a 1.43-Mev pulse. It can be seen that this effect is negligible in the data in Fig. 4, and it was also investigated with radioactive sources. In the spectra presented here it was standard practice to keep the counting rates low enough so that the effect was not significant.

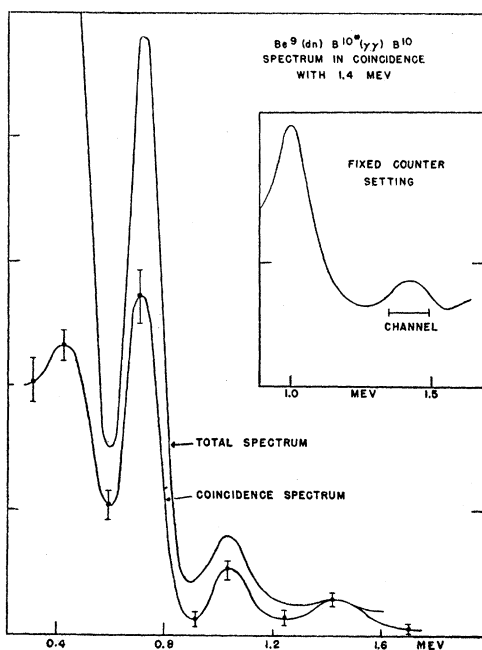


FIG. 6. Total spectrum and coincidence spectrum with the fixed channel set on the 1.43-Mev peak. The inset shows the total spectrum and fixed channel setting of the second counter.

Figures 5 and 6 give evidence for the existence of 1.43–1.02 Mev coincidences. The peak in the coincidence spectrum at 1.02 Mev is too strong and not properly located to be attributed to the Compton structure of 1.43-Mev radiation. To determine the effect of 2.15-Mev radiation in the fixed channel, a run was made with the channel set at 2.1 Mev. To within the statistical accuracy of the measurement, no 2.15–1.02 Mev coincidences were observed (i.e., the structure observed could be attributed to 2.15–1.43 Mev coincidences).

Figures 6 and 8 show a strong peak in the coincidence spectrum at 0.72 Mev. Part of this response can, of course, be attributed to 2.86–0.72 Mev coincidences, since the fixed channel is responding to some 2.86-Mev radiation. If, however, one counter is fixed on the 0.72-Mev peak, and the region around 1.4 Mev is searched with the other counter, a strong coincidence peak is obtained at 1.43 Mev, as shown in the inset in Fig. 5. In this case also, part of the response can be attributed to coincidences between 1.43-Mev gamma rays and other radiations. If there were no 1.43–0.72 Mev coincidences, however, either this peak or the one at 0.72 Mev (1.43 Mev fixed) would be expected to be weaker than observed.

In Fig. 8 the 1.43-Mev and 2.85-Mev curves are compared in the low energy region. At 0.41 Mev the 1.43-Mev curve rises above the 2.86-Mev curve, indicating the presence of 1.43–0.41 Mev coincidences.

C. Spectrum in Coincidence with 1.02-Mev Radiation

Figures 7 and 8 show the spectra obtained with the fixed channel set on the 1.02-Mev peak. The response at 1.43 Mev is due to the previously established 1.43–1.02 Mev coincidences. The relatively weak response at 1.0 Mev is interpreted as arising merely from the 1.43–1.02 Mev coincidences and the fact that either gamma ray can record in either channel. The strong peak at 0.72 Mev in Figs. 7 and 8 does not in itself establish 1.02–0.72 Mev coincidences. The strength of the peak at 1.02 Mev, when one channel is set on 0.72 Mev (see Fig. 9, or the inset in Fig. 5), however, makes these coincidences plausible.

The spectrum below 0.8 Mev is compared with the other spectra in Fig. 8. It is apparent that there is a very pronounced response from 1.02–0.41 Mev coincidences.

D. Spectrum in Coincidence with 0.72-Mev Radiation

Figure 9 shows the data obtained with the fixed channel on the 0.72-Mev peak. Comparing this curve with the curves in Fig. 8, it is seen that the rise at 0.4 Mev is significantly greater, as compared to the 0.72-Mev peak, with the fixed counter on 0.72 Mev than on any higher gamma ray, indicating the existence of 0.72–0.41 Mev coincidences. The coincidence response at 0.72 Mev in Fig. 9 is just about that which would be expected from coincidences between 0.72-Mev radiation and higher energy gamma rays (recorded in

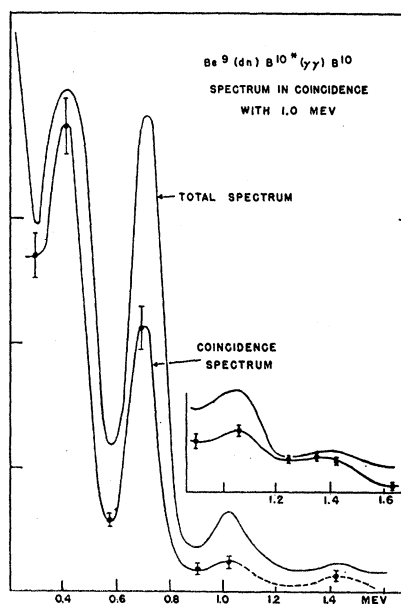


FIG. 7. Total spectrum and coincidence spectrum with the fixed channel set on the 1.02-Mev peak. The inset shows an independent run obtained with decreased gain and lower resolution.

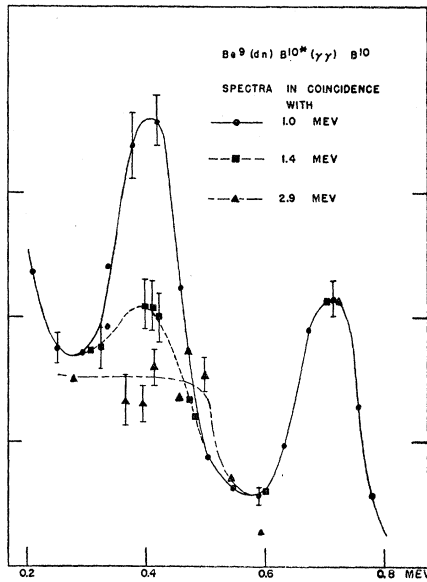


FIG. 8. Comparison of the 2.86-, 1.43-, and 1.02-Mev coincidence curves in the region of the 0.41- and 0.72-Mev peaks. These are independent runs not shown in the other figures. The 0.72-Mev curve in Fig. 9 may also be compared with these spectra, and the total spectrum in Fig. 9 is typical of the total spectra for the curves in this figure.

the 0.72-Mev channel). There is therefore no appreciable number of 0.72—0.72 Mev coincidences.

E. Decay Scheme

The decay scheme which is compatible with all these observations is shown in Fig. 10. It agrees with the scheme proposed by Ajzenberg,² except for the presence of the 1.43-Mev transition between the 3.58- and 2.15-Mev states. Recently, Dyer, and Bird⁴ have reported evidence for a state in B^{10} at 2.86 Mev. Since this state is not confirmed by the other investigations,^{2,3,5} it is shown as a dotted line. We cannot, of course, rule out an 0.72—2.86 Mev cascade involving this state, on the basis of the present work. Other possible transitions to or from the state are improbable from either the coincidence work or the observed gamma-ray spectrum.¹

Additional evidence for the existence of 1.43—1.43 Mev coincidences can be cited. The spectra in Figs. 5, 6, and 8 establish coincidences between the 1.43-Mev gamma ray and the 2.15-, 1.02-, and 0.41-Mev gamma rays. Hence, the “upper” 1.43-Mev transition between the 3.58- and 2.15-Mev states is well established. One may, however, consider the consequences of eliminating the “lower” 1.43-Mev transition between the 2.15- and 0.72-Mev states. Reference to the decay scheme in Fig. 10 shows that in that case the 1.43-Mev radiation should be equally strongly in coincidence with 0.41- and 0.72-Mev radiation. That this is not the case can be seen from Figs. 6 and 8. It can be ruled out not only on the basis of the relative efficiency of counting 0.41-

and 0.72-Mev radiation, but also by comparing the 1.43-Mev coincidence curve with the 1.02-Mev curve in Fig. 8.

Among the five states shown by solid lines, there are only two possible transitions which have escaped detection: the 1.84-Mev transition between the 3.58- and 1.74-Mev states, and the 1.74-Mev transition from the latter state to ground. With spin and parity assignments of 3^+ , 1^+ , 0^+ , 1^+ , and 2^+ for these five states taken in ascending order,^{2,5,9} the observed transitions are all of type $M1$ except for the 2.15- and 0.72-Mev radiations, which are $E2$. The latter transition is not in competition with any other radiation. The unobserved 1.84- and 1.74-Mev transitions are $E2$ and $M3$, respectively. The above assignments, therefore, are in reasonable agreement with the decay scheme.

V. ANGULAR CORRELATIONS

With the experimental arrangement described above, it was possible to obtain some information on angular correlations for various channel settings of the two counters. One counter was fixed at 90° to the beam direction, while the other counter was rotated in the plane containing the first counter and the beam. Each channel setting was selected so as to maximize the response from a particular gamma ray. The experimental arrangement and equipment were tested from time to time by measuring the well-established correlation between the Co^{60} gamma rays.¹⁰

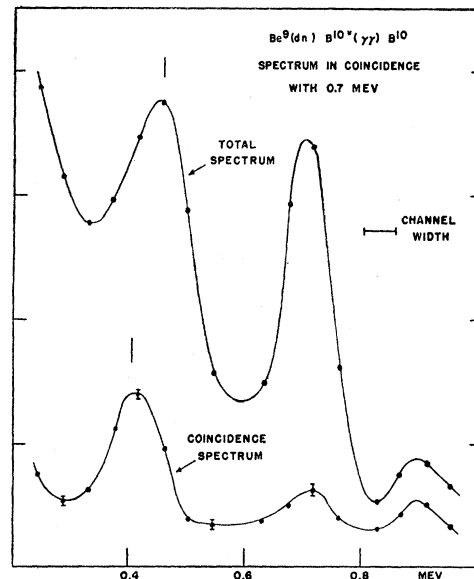


FIG. 9. Total spectrum and coincidence spectrum with the fixed channel set on the 0.72-Mev peak. The lowest peak in the total spectrum is a mixture of 0.41-, 0.48-, and 0.51-Mev radiations. Of these the coincidence spectrum selects only the 0.41-Mev gamma ray.

⁹ H. T. Richards, University of Pittsburgh Conference on Medium Energy Nuclear Physics, June, 1952 (unpublished).

¹⁰ E. L. Brady and M. Deutsch, Phys. Rev. 74, 1541 (1948).

The channel settings investigated are listed in Table I. For several of the gamma-ray pairs, the measurements were made first with one gamma-ray direction fixed and the second direction varying, and then with the roles of the gamma rays interchanged. In general different correlations will be observed in these two cases if the correlations are a function also of the beam direction. To within the accuracy of the measurements, significant differences were not observed in these cases.

In the angular data, no evidence was obtained for terms in the correlation functions higher than $\cos^2\theta$. Accordingly, after applying the necessary geometric corrections, a least square fit to each set of data was obtained with a function of the type $1+A_2\cos^2\theta$, where θ is the angle between the two gamma-ray directions. As can be seen from the table, the observed anisotropy in each case was not large, and the coefficients have not been corrected for the finite apertures of the detectors. Corrections arising from the motion of the radiating B^{10} nuclei are of the order of 1 percent or less and have not been included.

The 2.86–0.72 Mev pair is well isolated experimentally from other coincident radiations. With spin assignments of 2–1–3 to the participating states, a value of $A_2 \approx -0.08$ can be obtained theoretically

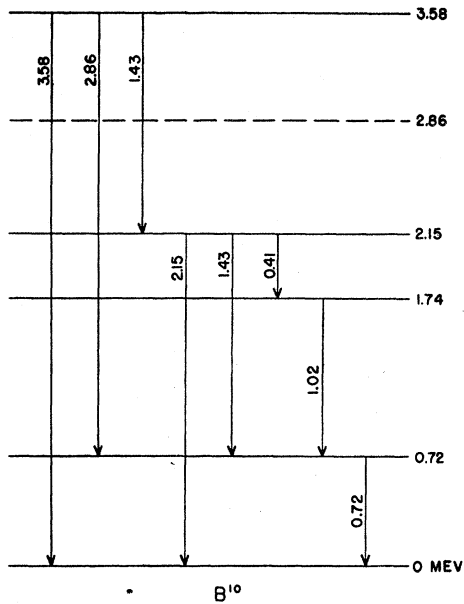


FIG. 10. The decay scheme in B^{10} which is compatible with the coincidence measurements.

TABLE I. Angular correlation coefficients. The first column indicates the channel setting of the counter fixed at 90° to the deuteron beam. The second column gives the channel setting of the other counter rotating in the plane containing the first counter and the beam. A_2 is the measured coefficient in the correlation function $1+A_2\cos^2\theta$, where θ is the angle between the counters. The errors include not only the statistical uncertainty, but also an estimate of the uncertainty arising from other sources.

Channel settings		A_2
Fixed (Mev)	Rotating (Mev)	
2.86	0.72	-0.08 ± 0.05
0.72	2.86	-0.07 ± 0.05
1.43	0.72	-0.08 ± 0.07
0.72	1.43	-0.14 ± 0.07
1.02	0.72	-0.09 ± 0.05
0.72	1.02	-0.10 ± 0.05
1.43	0.41	-0.13 ± 0.07
0.41	1.02	-0.06 ± 0.05
0.41	0.72	-0.03 ± 0.05

if the 2.86-Mev transition is a mixture of $M1$ and $E2$ radiation. For pure $M1$ radiation, the theoretical coefficient is -0.01 . For a 0–1–3 assignment one obtains $A_2 = -0.10$ uniquely.

The 1.43–0.72 Mev and 1.02–0.72 Mev measurements both give coefficients about equal to -0.10 . Since the former measurement provides a rough estimate of the effect of the background correlation in the latter observation, it may be concluded that the coefficient for the 1.02–0.72 Mev cascade is itself not greatly different from the measured value. The 1.43–0.72 process is complex, involving as many as three separate cascades (see Fig. 10), and the experimental measurement includes also some 2.86–0.72 Mev coincidences. For the 1.02–0.72 Mev process, however, a value of $A_2 = -0.10$ is expected with the spin assignments of 0–1–3.

The final measurements on the 0.41–1.43, 0.41–1.02, and 0.41–0.72 Mev settings may be discussed on the basis of Figs. 8 and 9. In the first measurement, the coincidences are due chiefly to the 0.72–1.43 Mev process, and the coefficient obtained is not inconsistent with the value found for the 0.72–1.43 Mev setting. In the other two measurements, on the other hand, the value of A_2 is reduced. It can be seen from Figs. 8 and 9 that in both these cases the coincidences involving the 0.41-Mev gamma comprise at least 50 percent of the observed yield. The smaller values found for A_2 , therefore, are consistent with the fact that both the 0.41–1.02 and 0.41–0.72 Mev correlations should be isotropic, since they involve the 1.74-Mev state, with zero spin, as an intermediate state.